*GEOLOGICA CARPATHICA*, OCTOBER 2023, 74, 5, 373–386 https://doi.org/10.31577/GeolCarp.2023.24

# Timing of Variscan syn-collisional metamorphism constrained by Lu–Hf and Sm–Nd garnet petrochronology (The Tatra Mountains, Western Carpathians)

MILAN KOHÚT[1,✉], ROBERT ANCZKIEWICZ[2] and MARCELINA BOCZKOWSKA[2]

[1]Earth Science Institute, Slovak Academy of Sciences, Dúbravská cesta 9, P.O. Box 106, 840 05 Bratislava, Slovakia; ✉milan.kohut@savba.sk
[2]Institute of Geological Sciences, Polish Academy of Sciences, Kraków Research Centre, Senacka 1, 31-002 Kraków, Poland

*(Manuscript received August 25, 2023; accepted in revised form December 11, 2023; Associate Editor: Igor Broska)*

**Abstract:** The Variscan high-pressure (HP) eclogite and medium pressure (MP) metapelitic gneisses from the Tatra Mts. crystalline basement (Western Carpathians, Slovakia) were dated by means of the Lu–Hf and Sm–Nd methods. The Lu–Hf and Sm–Nd garnet dating of mafic eclogite and metapelitic gneisses provides a new set of precise ages on Variscan syn-collisional metamorphism in the Western Carpathians. The published *P–T* conditions document peak eclogite facies metamorphism at 15–17 kbar and 650–695 °C, whereas garnet–sillimanite gneisses reached their climax at 5–6 kbar and 650–700 °C. Lu–Hf bulk garnet dating gave the precise ages of 354.5±1.2 Ma for eclogite, while the ages of 346.7±1.0 Ma and 345.9±1.0 Ma were determined for metapelites. The Sm–Nd dating of the same garnet fractions from metapelites gave the ages 344.9±2.6 and 345.4±9.3 Ma. Both the Sm–Nd and Lu–Hf ages are indistinguishable within their uncertainties, and so, when considering the major and trace element zonation in garnet, we interpret them as dating the time of prograde garnet crystallization. The data therefore indicates high-pressure, eclogite facies metamorphism in the Tournaisian, and medium-pressure metamorphism in Visean times. We interpret the eclogite facies metamorphism as a record of initial Variscan continental collision in the Early Carboniferous. Early metamorphism in the eclogite facies is a deeper expression of the subducting slab, and thus, garnet started to grow in eclogite ca. 10 Myr earlier than that in the sillimanite-bearing gneiss in a shallower level.

**Keywords**: Lu–Hf & Sm–Nd dating of garnet, eclogites, metapelites, Variscan orogeny, Western Carpathians, Tatra Mts.

## Introduction

The collision of continents is one of the most spectacular tectonic processes that leads to the formation of orogenic belts. Continental collision is characterized by deep subduction of continental crust, producing major crustal thickening, high-pressure/high-temperature (HP/HT) metamorphism, and anatexis of the subducted continental crust. The metamorphic rocks pressure–temperature–time (*P–T–t*) studies provide important information about the tectono-thermal evolution of the orogenic belts during burial and exhumation (England & Thompson 1984; Brown & Johnson 2018; Chowdhury et al. 2021 and references therein). Deciphering the evolution of continental collisional belts through time relies on the constraint of metamorphic rock histories in order to determine the temperature and pressure conditions at different times in different places within the orogen. Defining precise and reliable *P–T–t* paths require the linking of isotopic ages with mineral growth at specific metamorphic conditions. This is arguably achieved best by applying the dating of garnet, which participates in the vast majority of geothermobarometers used for determining the evolution of metamorphic conditions, including ultra-high temperature (UHT) and ultra-high pressure (UHP) episodes (Duchêne et al. 1997; Scherer et al. 2000; Anczkiewicz et al. 2004, 2007; Smit et al. 2013). Although the decoupling of major and trace elements at high temperature imposes some difficulties in interpreting the isotopic ages of garnet, trace element zonation trends in combination with experimental data on diffusion often allow for a precise link between ages and crystallization conditions (e.g., Anczkiewicz et al. 2007, 2012). In this study, we combined Sm–Nd and Lu–Hf garnet geochronology with *in situ* laser ablation ICP-MS trace element measurements in order to constrain evolution of the pre-Alpine basement of the Western Carpathians. We deliver high precision dating results of eclogite and metapelitic gneisses from the Tatra Mts., thereby providing new constraints on the Variscan continental collision process.

## Geological setting

The European Variscan and Alpine Mountain chains are typical collisional orogens. The Variscan orogeny was caused by the Himalaya type continental collision (e.g., Dewey & Burke 1973; Maierová et al. 2016) between Laurussia and Gondwana, forming the supercontinent of Pangaea. The Variscan belt resulted from the frontal north-directed amalgamation of a series of small microplates or 'terranes', which were progressively docked to the Laurussian margin during the Devonian to Carboniferous periods. The Alpine–Himalayan orogeny was caused by the continents of Africa and India colliding with Eurasia in the north, from the Cretaceous (western

branch) through the Paleocene, and to the Miocene up to the present (eastern branch; c.f. Froitzheim et al. 2008; Plašienka 2018). The Carpathians form part of an extensive orogenic belt spreading from the Atlas Mountains in Morocco through the Alps, Dinarides, Pontides, Zagros, and Hindu Kush to the Himalayas and China. The Western Carpathians are the northernmost, E–W trending branch of this Alpine belt, linked to the Eastern Alps in the west, and to the Eastern Carpathians in the east (Fig. 1A). The pre-Alpine basement of the Western Carpathians represents the easternmost exposure of the Variscan orogen in Europe. The correlation of Variscan and pre-Variscan basement rocks of the Western Carpathians with the pre-Mesozoic basement areas of the European Variscides and Alpine orogenic belts is still questionable due to a lack of precise age and compositional data of the metamorphic units. The nature and style of mid-crustal assembly and exhumation during continental collision has been previously investigated in the Tatra Mountains (Fig. 1B, C) of the Western Carpathians (e.g., Janák 1994; Janák et al. 1996, 1999; Poller et al. 2000; Moussallam et al. 2012; Burda et al. 2021). Most of the available geochronological data record the metamorphism and magmatism during the Variscan orogeny in the Late Devonian and Carboniferous periods (e.g., Poller & Todt 2000; Poller et al. 2000, 2001; Moussallam et al. 2012; Burda et al. 2013a, b, 2021; Gawęda et al. 2016, 2018; Kohút & Larionov 2021; Janák et al. 2022; Broska et al. 2022; Catlos et al. 2022; Maraszewska et al. 2022), when the major continents of Laurussia and Gondwana collided. Previous dating of eclogite zircons (Burda et al. 2021) has suggested that high-pressure metamorphism in the Tatra Mountains took place at ≥367 Ma, which is interpreted as subduction of oceanic crust, at least 20 Myr earlier than medium-pressure/high-temperature metamorphism at ca. 350–340 Ma recorded by the dating of monazite in sillimanite-bearing gneisses and migmatites (Janák et al. 2022). This is interpreted as a consequence of crustal thickening.

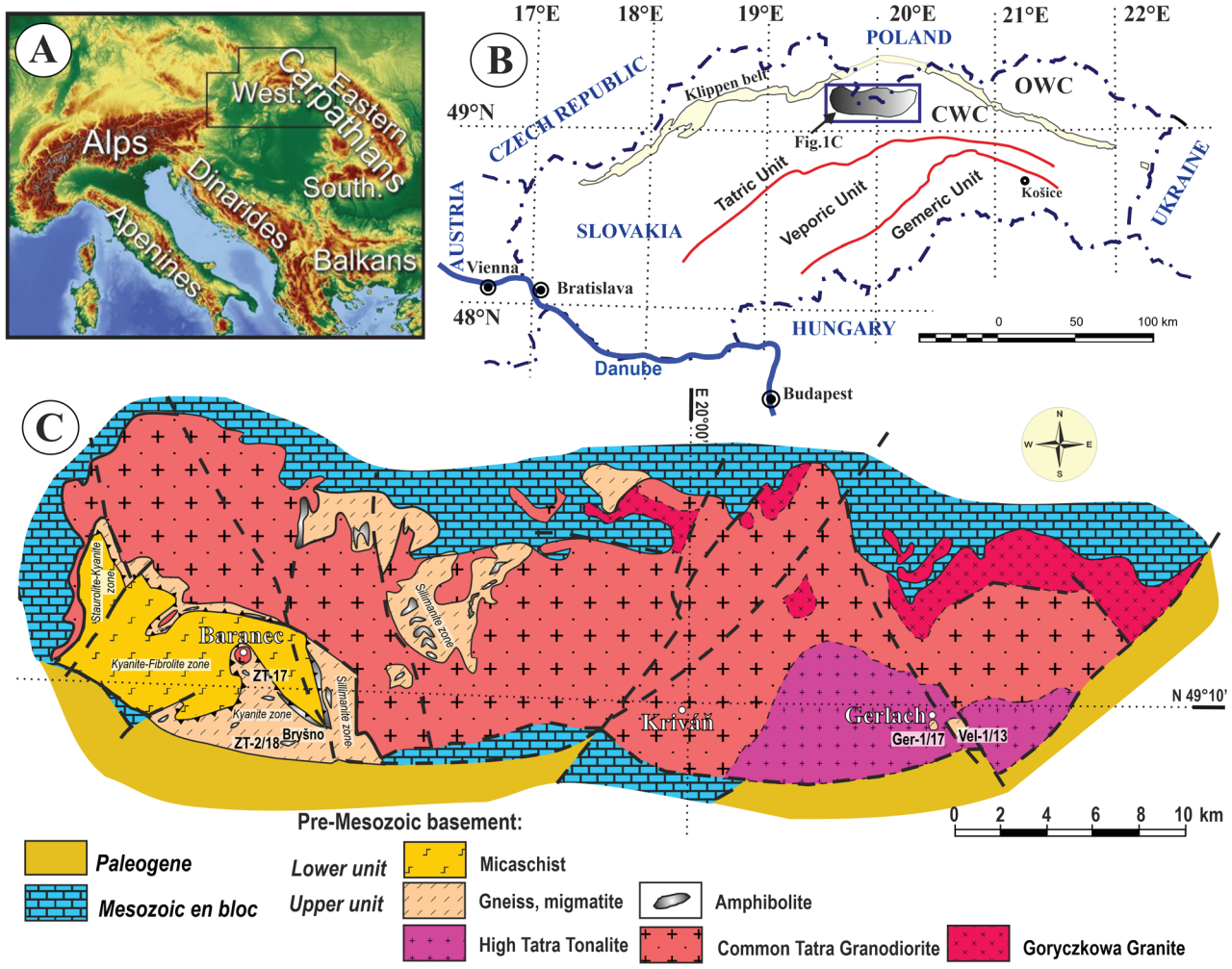


**Fig. 1. A** — A Digital Elevation Model (DEM) with position of the Western Carpathians within Europe. **B** — Tectonic scheme of the Western Carpathians with situation of the Tatra Mountains. *Abbreviations*: CWC – the Central Western Carpathians, OWC – the Outer Western Carpathians. **C** — Simplified geological map of the Tatra Mts., according to Kohút & Janák (1994) with locations of investigated samples. Metamorphic zonation taken from Janák et al. (1999).

The present-day structure of the Western Carpathians was derived from the Late Jurassic to Cenozoic (Alpine) orogenic processes connected with the evolution of the Neo-Tethys Ocean, in a long mobile belt sandwiched between the stable North European Plate and continental fragments of the African origin. One typical feature of the Alps–Carpathians mobile belt is the presence of the pre-Alpine crystalline basement within the Mesozoic and Cenozoic sedimentary successions, which had been deformed into large-scale nappe structures. The pre-Alpine crystalline basement crops out mainly in the Central Western Carpathians (CWC), which is the heart of the Western Carpathians. The CWC represents a pile of the Cretaceous thick- and thin-skinned thrust sheets, consisting of three principal crustal-scale superunits: the Tatric Unit, Veporic Unit, and Gemeric Unit (c.f. Andrusov 1968; Froitzheim et al. 2008; Plašienka 2018), see Fig. 1B.

The Tatra Mountains are located in the northernmost sector of the Western Carpathians. They are a representative of the so-called core mountains within the Tatric Unit, which is a major tectonic unit of the CWC. The crystalline basement of the Tatra Mts. is composed of pre-Mesozoic metamorphic and granitic rocks, overlain by Mesozoic and Cenozoic sedimentary cover sequences and nappes (Fig. 1C). Metamorphic rocks are abundant in the western part (the Western Tatra), whereas in the eastern part (the High Tatra), they occur as minor bodies in the granitic rocks (Fig. 1C). Two superimposed tectonic units – the Lower unit (LU) and Upper unit (UU), both differing in lithology and metamorphic grade, have been distinguished (Kahan 1969; Janák 1994; Janák et al. 1999). These units are separated by a Variscan thrust fault – a major tectonic discontinuity in the crystalline basement of the Tatra Mts. (Fig. 1C). The LU is exposed in the Western Tatra as a tectonic window of up to 1000-m thickness. It is composed of metapelitic micaschists with garnet, kyanite, staurolite, and fibrolitic sillimanite alternate with quartz-rich metapsammites and resembling flysch sediments (Kahan 1969). Metamorphic *P–T* conditions reached 5–6 kbar and 550–620 °C in the staurolite–kyanite zone and 6–8 kbar and 620–660 °C in the kyanite–sillimanite (fibrolite) zone (Janák 1994). The UU is composed of para- and orthogneisses, amphibolites, migmatites, calc-silicates, and granitoids. The paragneisses contain kyanite that is partly transformed to sillimanite at the base of the UU in the kyanite zone. Relics of eclogites occur as lenses or boudins in amphibolites. The presence of the meta-basic rocks with studied eclogites within the common felsic crustal rocks (e.g., orthogneisses and migmatized metapelites) and a general lack of ultramafites, serpentinites, and/or ophiolites in the studied area clearly indicate that continental crust was affected by the subduction/collision processes there. These amphibolites are often banded, with felsic layers of a trondhjemitic to tonalitic composition. Metamorphism in the kyanite zone reached eclogite facies at P>15 kbar and 700 °C followed by high-pressure granulite/high-pressure amphibolite facies overprint at ca. 10–14 kbar and 700–750 °C (Janák et al. 1996). Paragneisses with prismatic sillimanite (sillimanite zone) and rare cordierite occurs at higher levels of the UU. They show migmatization and partial melting due to dehydration reactions of muscovite and biotite at 6–10 kbar and 700–800 °C (Janák et al. 1999, 2022). Calc silicate rocks containing andradite–grossular garnet, diopside–hedenbergite clinopyroxene, epidote–clinozoisite, calcite and quartz occur only sporadically in the High Tatra, their metamorphic *P–T* conditions reached ca. 5 kbar and 650 °C (Janák 1993). Sillimanite zone gneisses and migmatites are intruded by a sheet-like granitoid pluton (Gorek 1959). Granitoids range from leucogranite to biotite tonalite and amphibolic diorite (Kohút & Janák 1994).

Polyphase Variscan and Alpine deformation under distinct *P–T* conditions and kinematics has been recognised (Fritz et al. 1992; Janák et al. 1999). The Variscan deformation (D1) under ductile conditions is demonstrated by kinematic indicators suggesting top-to-the-south, southeast thrusting and emplacement of the UU onto the LU. Variscan deformation (D2) is generally dextral, or top-to-the-east, related to orogen-parallel extension. Uplift and cooling took place between ca. 340–312 Ma, as recorded by Ar–Ar dating of biotite in metapelitic gneiss (Janák 1994) or biotite in the granitic rocks (Kohút & Sherlock 2003) in the High Tatra, and/or U–Pb zircon, titanite, and apatite dating of metamorphic rocks in the Western Tatra (Gawęda et al. 2018). Alpine deformation (D3) under brittle conditions is manifested by top-to-the-northwest shearing, which is attributed to a Late Cretaceous contractional event (Fritz et al. 1992).

Overall, metamorphic zonation in the Tatra Mts. displays an inverted sequence of high-grade metamorphic rocks and granitoids in the hanging wall, and lower-grade metamorphic rocks in the footwall. This is interpreted as a consequence of crustal thickening and mid-crustal thrusting in the course of Variscan orogeny (Janák et al. 1999, 2022).

## Analytical procedures

### *Garnet geochronology and trace element measurements*

Lu–Hf and Sm–Nd isotope dilution (ID) and trace element analyses were conducted at the Institute of Geological Sciences, PAS, Kraków Research Centre. The chemical protocols of ID analyses are given in Anczkiewicz et al. (2004) and references therein. The mass spectrometric measurements were conducted using the Multicollector Inductively-Coupled Plasma Mass Spectrometer (MC ICP-MS) *Neptune* according to the modified protocols of Thirlwall & Anczkiewicz (2004). Details on short- and long-term precision, as well as constants used for data reduction are reported in the footnote to Table 1. Ages were calculated using Isoplot v. 4 (Ludwig 2008) and are reported with 2σ uncertainty. Rim-to-rim trace element measurements were performed in order to facilitate garnet age interpretation. The analyses were conducted using *RESOlution* ArF excimer laser (Applied Spectra), equipped with a large format sample cell (S155, Laurin Technic). The laser ablation system was coupled with an ICP-MS/MS

**Table 1:** Summary of Lu–Hf and Sm–Nd garnet dating results. *Explanations*: Uncertainties on Hf and Nd isotope ratio measurements are 2SE (standard error). $^{176}Lu/^{177}Hf$ errors are 0.5 %, JMC475 Hf standard yielded $^{176}Hf/^{177}Hf=0.282156\pm3$ 2SD (standard deviation, n=10) over the course of analyses. Mass bias was corrected to $^{179}Hf/^{177}Hf=0.7325$; $^{147}Sm/^{144}Nd$ errors are 0.3 %, JNd-1 Nd standard yielded $0.512099\pm9$ (2SD, n=8) over the course of analyses. Mass bias was corrected to $^{146}Nd/^{144}Nd=0.7219$. Age calculations were conducted using Isoplot (Ludwig 2008) applying decay constants $\lambda^{176}Lu=1.865\times10^{-11}$ year$^{-1}$ (Scherer et al. 2001) and $\lambda^{147}Sm=6.02\times10^{-12}$ year$^{-1}$ (Lugmair & Marti 1978). Age calculations used uncertainties propagated for long-term standard reproducibility. Age uncertainties are 2σ.

| Fraction | Weight (mg) | Lu (ppm) | Hf (ppm) | $^{176}Lu/^{177}Hf$ | $^{176}Hf/^{177}Hf$ | 2SE | Age (Ma) | Sm (ppm) | Nd (ppm) | $^{147}Sm/^{144}Nd$ | $^{143}Nd/^{144}Nd$ | 2SE | Age (Ma) |
|---|---|---|---|---|---|---|---|---|---|---|---|---|---|
| **Eclogite ZT-2/18** | | | | | | | | | | | | | |
| WR | 98.78 | 1.111 | 0.605 | 0.2600 | 0.284603 | 0.000003 | | 7.469 | 22.04 | 0.2050 | 0.513079 | 0.000004 | |
| Grt 1 | 70.09 | 2.641 | 0.211 | 1.7730 | 0.294650 | 0.000008 | | 2.767 | 6.856 | 0.2441 | 0.513153 | 0.000006 | |
| Grt 2 | 72.85 | 2.600 | 0.190 | 1.9370 | 0.295728 | 0.000009 | | 2.653 | 6.494 | 0.2470 | 0.513163 | 0.000008 | |
| Grt 3 | 71.50 | 2.622 | 0.192 | 1.9340 | 0.295734 | 0.000008 | **354.5±1.2** | 2.733 | 6.668 | 0.2478 | 0.513163 | 0.000006 | **298±43** |
| **Metapelite Ger-1/17** | | | | | | | | | | | | | |
| WR | 100.10 | 0.412 | 0.329 | 0.1770 | 0.283599 | 0.000005 | | 7.297 | 34.94 | 0.1262 | 0.511953 | 0.000002 | |
| Grt 1 | 68.84 | 9.284 | 0.386 | 3.4160 | 0.304611 | 0.000006 | | 0.545 | 0.899 | 0.3664 | 0.512487 | 0.000007 | |
| Grt 2 | 70.23 | 9.285 | 0.372 | 3.5410 | 0.305502 | 0.000006 | | 0.455 | 0.239 | 1.1541 | 0.514269 | 0.000016 | |
| Grt 3 | 71.04 | 9.187 | 0.333 | 3.9200 | 0.307871 | 0.000008 | **346.7±1.0** | 0.524 | 0.560 | 0.5659 | 0.512958 | 0.000013 | **344.9±2.6** |
| **Metapelite Vel-1/13** | | | | | | | | | | | | | |
| WR | 98.80 | 0.445 | 0.228 | 0.2760 | 0.284308 | 0.000011 | | 7.911 | 42.97 | 0.1113 | 0.511915 | 0.000002 | |
| Grt 1 | 70.69 | 7.300 | 0.468 | 2.2140 | 0.296875 | 0.000005 | | 0.553 | 1.159 | 0.2883 | 0.512318 | 0.000007 | |
| Grt 2 | 71.42 | 7.491 | 0.479 | 2.2160 | 0.296859 | 0.000003 | | 0.514 | 0.994 | 0.3123 | 0.512368 | 0.000006 | |
| Grt 3 | 72.15 | 7.318 | 0.502 | 2.0650 | 0.295906 | 0.000005 | **345.9±1.2** | 0.629 | 1.450 | 0.2620 | 0.512256 | 0.000005 | **345.4±9.3** |

*Agilent* 8900. The data were collected in line scan mode with a 0.5 mm/min stage speed, spot diameter of 40 µm, 10 Hz pulse repetition rate, and 6 J/cm$^2$ energy. More details on analytical parameters are provided in Supplementary Table S1. Sample runs were bracketed by measurements of NIST 612 glass using reference values of Jochum et al. (2011). The BCR-2 glass standard was measured for the quality control adapting recommended values of GeoReM (http://georem.mpch-mainz.gwdg.de/). The silica concentration was used as an internal standard. Trace element concentrations were calculated using the Iolite 4 software (Paton et al. 2011).

### *Sample locations*

The investigated rocks are eclogite and sillimanite-bearing metapelitic gneiss. The eclogite comes from the kyanite zone in the Western Tatra, which is the lowest structural level within the UU where eclogites and gneisses containing kyanite are partly transformed to sillimanite, and record the highest pressure conditions in the Tatra Mts. (Janák et al. 1996, 1999). The eclogite sample ZT-2/18 was collected as a loose block from the creek in the Bryšno Valley (49°08'03.4"N; 19°45'46.9"E) at the southern slopes of Baranec (Fig. 1C). The metapelitic gneisses come from the sillimanite zone in the High Tatras, the highest structural level of the UU that does not host eclogites. The samples were collected from the two localities (Fig. 1C): Gerlach peak (sample Ger-1/17) and the Velická Valley (sample Vel-1/13). Sample Ger-1/17 (49°09'40.8"N; 20°08'09.9"E) crops out near the peak of Mt. Gerlach (see Janák et al. 2022), which is the highest peak of the Tatra Mts. (altitude 2655 m). The metapelitic gneiss crops out together with calc-silicate rocks (altitude 2500–2550 m), as layers of 2–15 meters thickness in granodiorite. Sample Vel-1/13 (49°09'35.0"N; 20°09'26.2"E) occurs as a band of several tens of meters thick in granodiorite, in the Velická Valley (see Janák et al. 2022). The outcrops show typical metamorphic foliation dipping 40–60° N, NW with lineation and b-axis of folds in a N–S and NW–SE direction.

## Results

### *Petrography and mineral chemistry*

#### *Eclogite*

The investigated eclogite (sample ZT-2/18) shows a dark-green, amphibole-rich texture with reddish garnet and a pale green clinopyroxene (Fig. 2A). A detailed description of this sample comes from the work of Janák et al. (1996). *Garnet* forms euhedral to subhedral grains (3–10 mm in diameter), which are surrounded and partly resorbed by an amphibole–plagioclase kelyphitic rim (Fig. 2B). Garnet contains numerous inclusions found mostly in the core. The most abundant inclusions are quartz, rutile, and ilmenite with subordinate

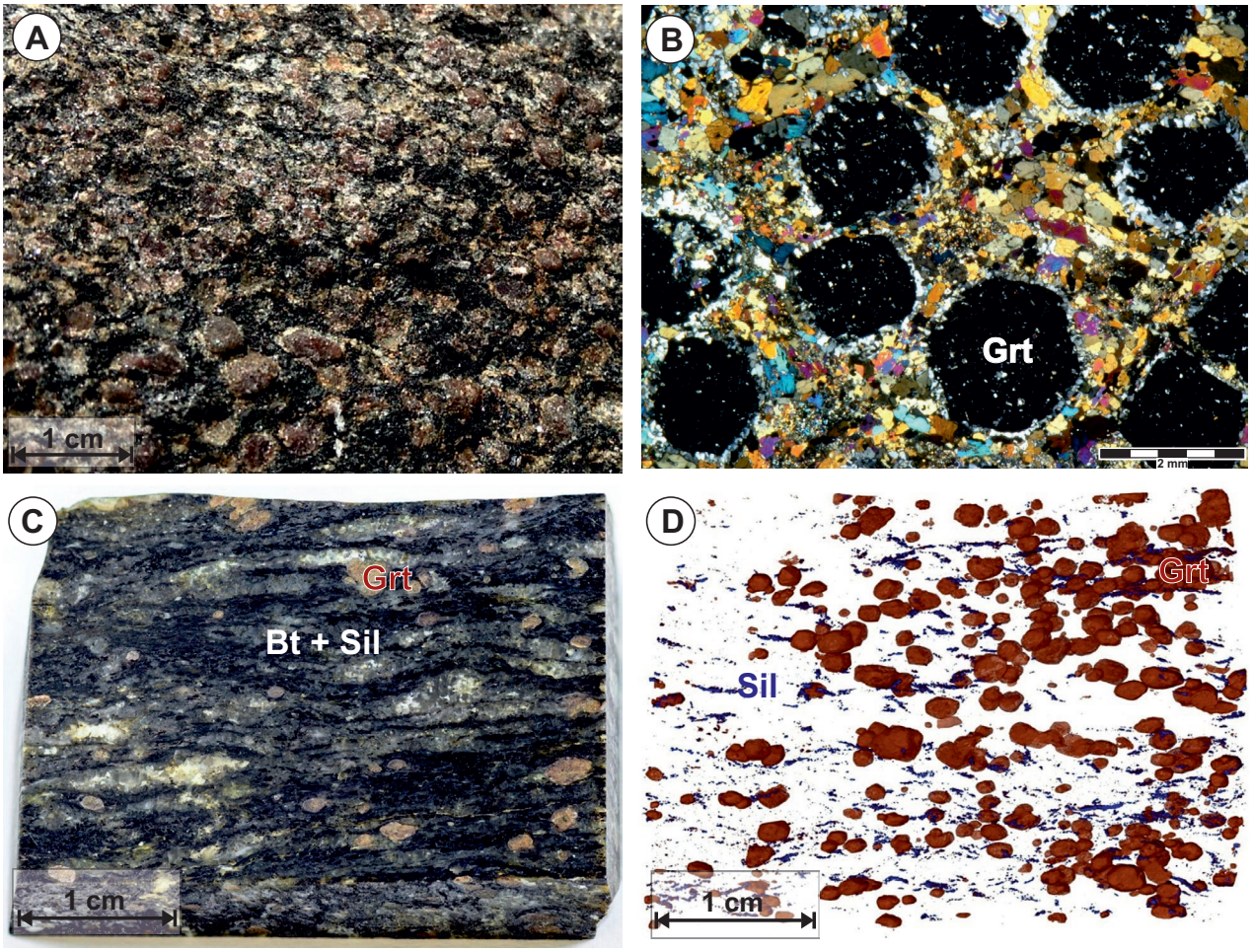


**Fig. 2**. **A** — Macrophotograph of eclogite sample ZT-2/18 documenting the quantity and size of analysed garnets. **B** — Microphotograph of eclogite sample ZT-2/18 showing texture of the euhedral garnets (black) with pale inclusions and kelyphitic rims. **C** — Macrophotograph of metapelitic gneiss (Ger-1/17) with garnet visible on the surface. **D** — Micro-CT image of identical metapelitic gneiss plate as in Fig. 2C with garnet (terracotta) and sillimanite (blue) visible in 3D.

plagioclase, amphibole, clinopyroxene, epidote/zoisite, apatite, and zircon. The garnet is zoned, showing an increase in Mg and Fe and a decrease in Mn from the core to the rim, which corresponds to almandine with significant grossular and pyrope contents, and is also characteristic of prograde growth zoning. In the outermost part of the rim, Mn and Fe rise, whereas Mg drops as a result of resorption (see fig. 4 in Janák et al. 1996). *Clinopyroxene* occurs mostly as symplectite with plagioclase, which is often recrystallised to granoblastic aggregates where amphibole is also present. The composition of symplectitic clinopyroxene is diopside ($X_{Jd} \leq 0.05$). On the basis of the modal proportions of clinopyroxene and plagioclase in symplectites, Janák et al. (1996) reconstructed the "primary" clinopyroxene composition as omphacite with a jadeite content of 36 mol. %, thus implying a peak-pressure of 15–17 kbar. *Amphibole* is the most abundant phase that occurs as inclusions in garnet, as well as in kelyphites with plagioclase and symplectites with clinopyroxene and plagioclase, including porphyroblasts in the matrix. The composition of these amphiboles corresponds to pargasite, tschermakite, and Mg-hornblende; actinolite formed as a late phase in fractures. *Plagioclase* occurs in symplectites with clinopyroxene and amphibole, as well as in kelyphitic rims around garnet and as minor inclusions in garnet. *Rutile* and *ilmenite* are abundant in the matrix and *titanite* in the most retrograded domains. For more details, see Janák et al. (1996).

*Metapelitic gneisses*

The rock texture is medium-grained, the foliation is defined by the preferred orientation of biotite and quartz–feldsphatic portions, which form felsic layers and segregations. A comprehensive description of the studied metapelitic gneisses comes from the works of Janák et al. (1999, 2022). The rocks contain garnet, sillimanite, biotite, muscovite, quartz, and plagioclase as major mineral phases (Fig. 2C, D). Minor and accessory minerals include tourmaline, apatite, zircon, and monazite. Rutile has been partially or totally replaced by ilmenite.

Prismatic sillimanite and biotite are mostly oriented parallel to foliation, whereas muscovite often crosscuts the foliation. Garnet encloses prismatic sillimanite, biotite, white mica, quartz, staurolite, zircon, apatite, monazite, and ilmenite (with remnants of rutile). Most inclusions are located in the core of the studied garnet. Some garnets are fractured, truncated, or partially resorbed by biotite (often chloritized) at their margins and in pressure shadows, while fractures are filled by chlorite. Felsic layers are composed of plagioclase and quartz. Neither K-feldspar nor partial melting has been observed in the investigated gneisses. *Garnet* porphyroblasts are zoned with respect to composition (see Janák et al. 1999, 2022). Microprobe analyses of selected grains show in the garnet core a decrease in spessartine and a slight increase in pyrope, whereas a reverse pattern is observed in the rim of garnet; there is a marked Mn enrichment in contact with biotite. These compositional patterns indicate that prograde growth zonation of garnet was modified by diffusion and retrograde net-transfer reactions with biotite. *Biotite* occurs as inclusions in garnet and in the matrix; muscovite porphyroblasts in the matrix show a moderate phengite component. Some inclusions in garnet show a higher phengite content, and paragonite was also detected (Janák et al. 2022). *Plagioclase* (An=0.23–0.24) is present in the matrix; no feldspar was found as an inclusion in garnet. *Staurolite* enclosed in garnet is Fe-rich ($X_{Fe}$=0.78) with a zinc content of 2.2 wt. %. For more details, see Janák et al. (1999, 2022).

### *Lu–Hf and Sm–Nd garnet dating*

A summary of Lu–Hf and Sm–Nd garnet dating is presented in Table 1 and Fig. 3. All isochrons are defined by 3 garnet separates, as well as the representative whole rock (WR) fraction. Lu–Hf dating of eclogite ZT-2/18 gave its age of 354.5±1.2 Ma. Dating of metapelites resulted in similar precision ages: 346.7±1.0 Ma was obtained for sample Ger-1/17, while 345.9±1.2 Ma was determined from Vel-1/13. The corresponding Sm–Nd ages are 298±43 Ma, 344.9±2.6, and 345.4±9.3 Ma respectively. All Lu–Hf ages are precise and accompanied by low MSWD, ranging from 0.2 to 0.7. Their Sm–Nd counterparts show either lower or very low precision (in the case of ZT-2/18 eclogite), with MSWD ranging from 0.4 to 4.4. Details of the observed isotope systematics in the context of trace element distribution in garnet is discussed in chapter "Garnet geochronology".

## Discussion and conclusions

### *Pressure and temperature conditions*

*P–T* conditions of the investigated eclogite sample ZT-2/18 were adopted from the published work of Janák et al. (1996) and determined by conventional geothermobarometry. According to Janák et al. (1996), the peak *P–T* conditions in eclogites reached ca. 15–17 kbar and 675–695 °C. Major element zoning indicates that despite resorption in the rims, eclogite garnet grew during prograde metamorphism.

The *P–T* conditions of the garnet-bearing sillimanite paragneisses samples Ger-1/17 and Vel-1/13 were implemented from the published works of Janák et al. (1999, 2022). Pressure–temperature results indicate the peak of prograde growth of garnet in both metapelite samples within the stability field of garnet+sillimanite+plagioclase+biotite+muscovite+ilmenite+quartz with the *P–T* values to 5–6 kbar and 650–700 °C (see Janák et al. 2022).

### *Garnet geochronology*

Our garnet dating results provide a rather coherent set of Lu–Hf ages Sm–Nd ages. In general, the lower precision of the Sm–Nd ages is a result of smaller spread among $^{147}Sm/^{144}Nd$ ratios in comparison to $^{176}Lu/^{177}Hf$ ratios. This is due to the fact that garnet generally fractionates Sm/Nd to a much lesser degree than Lu/Hf. Additionally, *in situ* trace element analyses revealed that garnet isotope dilution (ID) analyses of sample ZT-2/18 were overwhelmed by the presence of Nd-rich inclusions, which did not allow us to obtain a high-quality age. While laser ablation ICP-MS analyses indicate sub-ppm concentration in pure garnet (Fig. 4), ID analyses recorded a 6–7 ppm Nd concentration (Table 1). The Nd rich domains in garnet from the eclogite correlate with the U, Th, and light REE enrichment, which suggests a significant contribution of apatite, but possiblly epidote inclusions as well (Supplementary Fig. S1). The strong departure of the obtained Sm–Nd age from all other ages may suggest the presence of the inherited minerals, which shifted the "isochron age" towards younger values. However, within its low precision, this age is still the same as the ages of garnet from metapelites. Garnets from the two metapelitic gneisses were also affected by inclusions, although to a much lesser extent. While "pure garnet" records Nd concentration within a sub-ppm range (Fig. 4), ID analyses document 5 times higher level (Table 1). Laser ablation ICP-MS rim-to-rim zonation profiles show the rise in Nd concentration concomitant with the rise in Th, U, and light REE, pointing to apatite as the main reason for the disturbed Sm–Nd systematics in garnet. Although contribution from inclusions to Sm–Nd budget lowered age precision, the consistency of Sm–Nd and Lu–Hf ages in metapelites indicates that the accuracy was not jeopardized.

Although Lu–Hf isochrons are of high quality, they also suffer from the inclusion problem. While bulk separate ID measurements reproduce the average Lu content in garnet estimated by LA ICP-MS, Hf concentration is higher than expected for pure garnet (Table 1, Fig. 4). *In situ* analyses point to about 0.100–0.200 ppm Hf concentration, whereas ID data show values from 0.2 to 0.6 ppm. This is most likely due to the presence of titanite. Although zircon and rutile also carry a significant amount of Hf, they contribute less to the Hf budget due to their refractory nature and very limited solubility during hot plate sample digestion. Most importantly, fairly high $^{176}Lu/^{177}Hf$ ratios and a very good fit of the isochrons

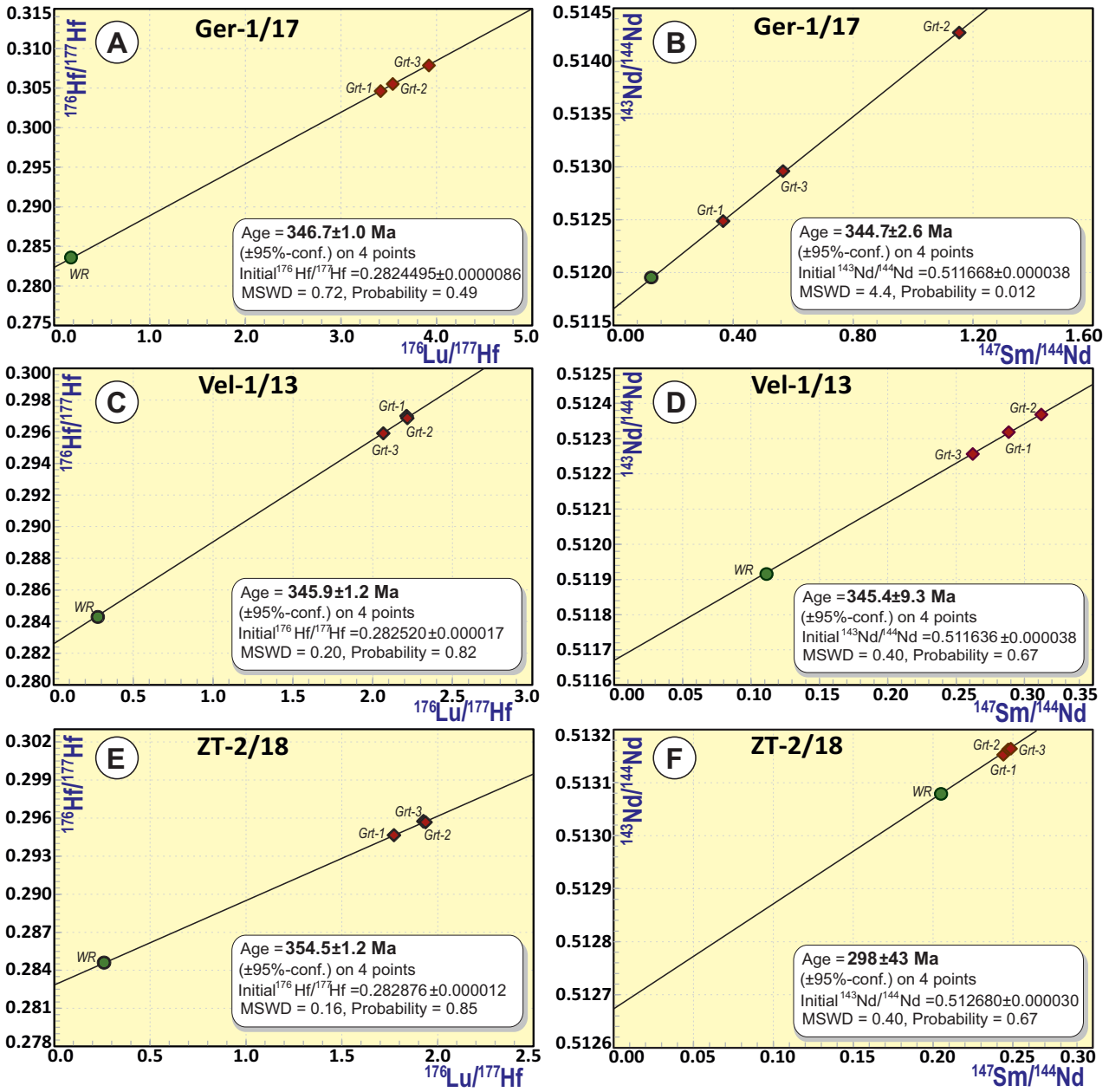


**Fig. 3**. Lu–Hf and Sm–Nd isochron diagrams of samples from the Tatra Mts. *Abbreviations*: WR – whole rock, Grt – garnet. Errors are smaller than the size of the used symbols. See text for details.

(MSWD ranging from 0.2 to 0.7) demonstrate that the inclusions were in equilibrium with garnet, and the ages were affected only in terms of precision, but not accuracy.

All dated samples formed at similar temperatures (650–700 ºC) and, as described above, they preserved prograde major element zonation (see Janák et al. 1996, 1999, 2022). Since the diffusivities of REE and Hf are much slower than those of the major divalent cations, they also are interpreted as reflecting prograde garnet growth. The zonation style of elements involved in both geochronometers is known to affect ages (Lapen et al. 2003). Preferential partitioning of Lu towards garnet core tends to shift the Lu–Hf age towards the early phase of mineral growth, whereas Nd and Sm tend to be enriched in rims shifting the age towards a later crystallization phase. Rim-to-rim profiles in metapelite Vel-1/13 does show some zonation, yet rather atypical in the case of Sm, which shows enrichment in a broad core similarly to Lu. There is some clear Lu enrichment in the narrow rims, which is most likely due to resorption; however, they are volumetrically minor and unlikely to significantly affect dating results. Both Lu–Hf and Sm–Nd ages are indistinguishable within their uncertainties, and thus, we interpret them as dating of the time of prograde garnet crystallization. In the case of Ger-1/17 gneiss, there are no zonation trends. Lu concentration

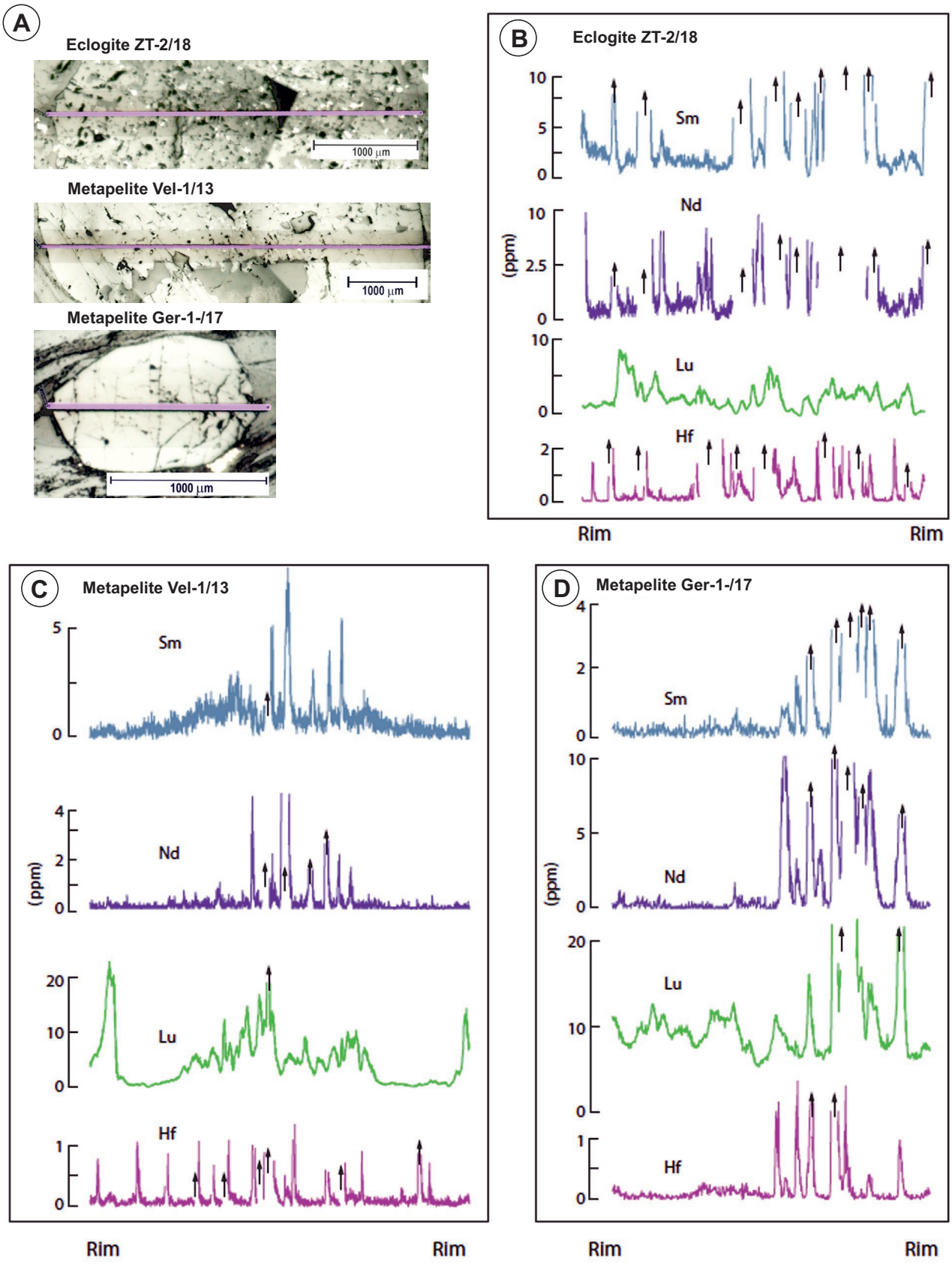


**Fig.4**. Rim-to-rim zonation of Sm, Nd, Lu and Hf concentration in representative garnets. **A** — Photomicrographs of the measured garnets with the marked line traverses; **B** — Eclogite ZT-2/18; **C** — Metapelite Vel-1/13; **D** — Metapelite Ger-1/17. Black arrows indicate the rise of concentration beyond the scale.

fluctuates across the crystal, whereas Sm is fairly uniform. Unfortunately, the quantity of inclusions in the garnet cores is too high to make any conclusions about the potential zonation trend in that region. The 346.7±1.0 Ma Lu–Hf and 344.9 ±2.6 Ma Sm–Nd ages are the same within their uncertainties, thus indicating that the observed trace element zonation did not cause the commonly observed decoupling of the two isotopic clocks within the obtained precision (Fig. 4, Suppl. Fig. S1, Table 1). Both ages are interpreted as reflecting the average age of garnet crystallization on a prograde path. When taking into consideration that the Nd, Sm, Lu, and Hf zonation gradient is not very strong, the obtained ages are not very far from the temperature peak.

### *Dating of the HP and MP rocks in the Tatra Mts. – comparison of available data*

The U–Th–Pb dating of magmatic zircon cores indicates the crystallization age of a basaltic magmatic precursor of eclogitic boudins at ca. 600–560 Ma (Gawęda et al. 2017) and ca. 503–480 Ma (Putiš et al. 2009; Burda et al. 2021) within the CWC. The Lu–Hf and Sm–Nd dating of eclogite and metapelitic gneisses from the Tatra Mts. presented in this study provides a new set of accurate and precise ages on Variscan metamorphism in the Western Carpathians. Lu–Hf dating of eclogite resulted in 354.5±1.2 Ma age of prograde eclogite facies metamorphism. We did not manage to obtain precise Sm–Nd age for eclogite (298±43 Ma), however, Moussallam et al. (2012) dated eclogite collected near the Baranec summit to 337.2±9.9 Ma using isotope dilution and Thermal ionisation mass spectrometry (ID-TIMS). The authors interpreted the latter age as post-eclogite, retrograde garnet re-equilibration.

All four ages obtained for metapelites define the time of prograde garnet growth at about 346 Ma. These data suggest that high-pressure, eclogite facies metamorphism occurred in the Tournaisian, while medium-pressure metamorphism took place in the Visean (both Early Carboniferous) times (Fig. 5). Due to differences in rheology and rock composition, the eclogite garnets Lu–Hf isotopic system was closed during its maximum burial at HP conditions, whereas the metapelites recorded their maxima growth at the mid-crustal conditions. Also worthy of consideration is the medium-pressure/high-temperature metamorphism between ca. 350–340 Ma, which was recorded similarly by dating of zircon and monazite in sillimanite-bearing gneisses and migmatites (Moussallam et al. 2012; Janák et al. 2022). Both metapelite samples from the present study were dated also by the monazite Th–U–Pb method with 350–345 Ma ages (Janák et al. 2022). Interestingly, two groups of monazites were identified in the sample Ger-1/17. The low-Y monazite, which shows an age of 356.5±6 Ma (Mnz-1), may have reflected an older metamorphic event at higher-P (ca. 7.5 kbar), whereas the high-Y monazite, which gives an isochron age of 345.8±6 Ma (Mnz-2), recorded younger MP/HT metamorphism M2 according Janák et al. (2022).

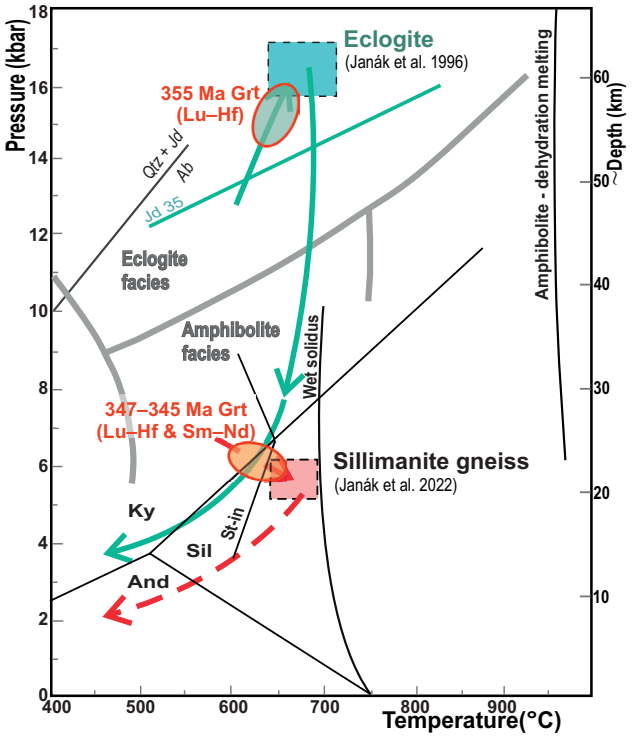


**Fig. 5**. Metamorphic conditions and *P–T* paths of the Tatra Mts. Upper unit. Metamorphic conditions and *P–T* path of eclogite (green box, green arrow) from Janák et al. (1996). Metamorphic conditions and *P–T* path (pink box, red dashed arrow) of the sillimanite gneisses from Janák et al. (2022). Prograde garnet growth (green/red ellipsoid) reflects eclogite Lu–Hf age data, and garnet growth in sillimanite gneisses (red ellipsoid) represents Lu–Hf & Sm–Nd ages, both are from this study. ~Depth deduced from a mean crustal density of 2800 kg m$^{-3}$.

Previous LA-MC-ICP-MS amphibolite zircon U–Pb age data from the Polish part of the Western Tatras indicated the parent mantle-derived basaltic magma crystallization at ca. 560 Ma, with potential high-pressure metamorphic overgrowth at ca. 387–372 Ma and a younger (medium-pressure) event at ca. 342–338 Ma (Gawęda et al. 2017). Later, Gawęda et al. (2018) dated amphibolite U–Pb zircons from the northern Polish part of the Western Tatra with two age populations: (1) 385 Ma and (2) 346 Ma, while the apatites from identical amphibolite samples gave an age of 351.8±4.4 Ma. Although the titanites from amphibolite from the southern Slovak part of the Western Tatras yielded a U–Pb age of 345.3±4.5 Ma, Gawęda et al. (2018) thus interpreted the age of ca. 345 Ma as the climax of metamorphism and the onset of immediate exhumation of the entire Tatra Mts. Recent Secondary Ion Mass spectrometry (SIMS) U–Pb zircon age data from the eclogite in the Western Tatras (Baranec) by Burda et al. (2021) recorded two zircon forming events: (1) ≥367 Ma, interpreted by Burda et al. (2021) as a minimum age for eclogite facies metamorphism, and (2) 349 Ma, interpreted as retrogression under amphibolite facies conditions.

Very little is known about the age of the Variscan metapelite (MP) metamorphism in the Western Carpathians. The published Rb–Sr WR isochrons and WR–biotite pairs (ca. 355–351 Ma) from the Malé Karpaty Mts. biotite gneisses (Tatric Unit) have shown ages that are coeval and/or slightly predate the intrusion of the Variscan granitic rocks (Bagdasaryan et al. 1983). Considerable thermal overprint by the extensive Variscan migmatization/ granitization onto the CWC metamorphic rocks caused the available K–Ar and Ar–Ar muscovite and biotite cooling ages (ca. 335–312 Ma with sporadic maxima at 345 Ma) to reflect ultimate exhumation of the entire CWC due to extension and unroofing of the basement formed by the Variscan orogeny (Bagdasaryan et al. 1977; Maluski et al. 1993; Janák 1994; Dallmeyer et al. 1996). Recently, Gawęda et al. (2018) presented apatite U–Th–Pb dating of biotite paragneiss from the metamorphic basement of the Western Tatra Mts. with an age of 342.6±7.1 Ma; the authors proposed a metamorphic climax at ca. 345 Ma and contemporaneous metapelites anatexis due to rapid exhumation. Interestingly, almost all of the recent results of geochronometry, including our data, indicate the medium-pressure/ high-temperature metamorphism of metapelites and/or their migmatization between ca. 350–340 Ma in the Tatra Mts. When taking into consideration the aforementioned age data sets (Gawęda et al. 2017, 2018; Burda et al. 2021), there would be an age gap of at least 20 Myr between the HP metamorphism and the MP/HT metamorphism in the Tatra Mts. However, zircon commonly grows only during pre-HP prograde or during retrograde amphibolite-facies conditions in similar tectonic environments and mechanisms; indeed the subduction–exhumation events appear to be discrete, discontinuous, and last <ca. 10 Ma (Warren 2013). It is also worth mentioning that the Lu–Hf and Sm–Nd age data presented in this study indicate that the time span between the HP and MP metamorphism was ~10 Myr in the Tatra Mts. Earlier metamorphism in the eclogite (ca. 355 Ma) can be the expression of a deeper position within the subducting slab and thus, eclogite garnet started to grow ca. 10 Myr earlier than garnets in the sillimanite-bearing gneiss at a shallower level.

### *Comparison with the surrounding areas*

Eclogite facies metamorphism is known from all three principal parts of the CWC – the Tatric, Veporic, and Gemeric units (e.g., Janák et al. 1996, 2007, 2009; Janák & Lupták 1997; Faryad et al. 2005, 2020). Albeit, the presented Lu–Hf garnet dating of the eclogite facies metamorphism is the first from the Western Carpathians.

The Western Carpathians geological structure is comparable to the Eastern Alps. However, a number of eclogite localities were recognised within the Alps; they show either a Variscan or Alpine age of HP (UHP) metamorphism. The Lu–Hf garnet dating study showed that the majority of eclogites from the Austroalpine high-pressure belt (Saualpe/Koralpe, Schobergruppe, Sieggraben, Texelgruppe, and Pohorje localities) yielded prograde garnet growth ages between 101.79±0.92 Ma and 89.89±0.37 Ma, suggesting a short period of (ultra) high-pressure metamorphism (Miladinova et al. 2022). However, the recent Lu–Hf dating of eclogite garnets from the Schobergruppe revealed, in addition to the Alpine ages (ca. 97 Ma), a Variscan ca. 313–300 Ma age of eclogitization as well (Hauke et al. 2019). Similar scattered relics of Variscan eclogite facies metamorphism were identified in other parts of the Austroalpine basement, e.g., in the Ötztal Nappe (347±9 Ma; Miller & Thöni 1995), Silvretta Nappe (351 ±22 Ma; Ladenhauf et al. 2001), and Ulten Zone (336.1 ±4.4 Ma; Tumiati et al. 2003). Eclogitized metagabbros yielded the Sm–Nd isochron protolithic ages between ca. 275 and 247 Ma for the Saualpe/Koralpe samples (Thöni & Jagoutz 1992; Miller & Thöni 1997). Similarly, combined zircon U–Pb dating, whole rock geochemistry, and Hf isotope analysis revealed that the eclogite samples for the Saualpe/Koralpe and Sieggraben samples predominantly show the Permian to Middle Triassic protolith ages of ca. 253–241 Ma (Chang et al. 2022, 2023).

The Bohemian Massif, as a part of the stable European Variscan belt, is characterised by the abundant presence of eclogites and/or HP (UHP) products within the Saxothuringian, Teplá–Barrandian, and Moldanubian units. Distinct phases of HP (UHP) metamorphism from the mid Devonian through to the Carboniferous were identified due to oceanic and continental subduction and subsequent exhumation. The mid-Devonian phase (ca. 400–380 Ma) mirrored the eclogite facies conditions before a pervasive granulite facies overprint (e.g., O'Brien 1997; Anczkiewicz et al. 2007; Collett et al. 2018). A second phase was characterised by blueschist- to eclogite-facies metamorphism in the Late Devonian and Early Carboniferous (ca. 360–350 Ma; e.g., Schmädicke et al. 2018; Konopásek et al. 2019). However, the third phase was associated with spectacular occurrences of Carboniferous (ca. 355–335 Ma) UHP and ultra-high temperature (UHT) assemblages (e.g., Medaris et al. 2006; Ackerman et al. 2016).

Unlike the HP eclogite facies metamorphism, there is a lack of real geochronological data for the mid-crustal metapelites (MP or MP/HT gneiss) metamorphism in Central Europe. Since recent Lu–Hf garnet data are lacking in the Alps, the Variscan metapelite metamorphosis was deduced often from the U–Th–Pb, Sm–Nd, or Rb–Sr isotopic determinations. Geochronological data (Rb–Sr WR isochrons and white micas Ar–Ar data) support the existence of a two-stage development of the Variscan metamorphism of the acidic metavolcanic rocks and quartz-phyllites from the Eastern Southalpine basement. The first stage at about 350 Ma has been related to the early regional heating, whereas the second stage at 330–325 Ma likely dates the thermal climax (Del Moro et al. 1980; Meli 2004). The Variscan metapelite metamorphism reached amphibolite facies, and its peak age was well constrained by Sm–Nd WR–garnet ages of 343–331 Ma (Hoinkes et al. 1997) and EMPA CHIME monazite ages of 335–320 Ma (Schulz 2021) from the Ötztal-Stubai Complex in the Western Austroalpine. The stromatic gneisses yielded WR–garnet Sm–Nd age, which indicates an isotopic homogenization

event at 330.4±4.4 Ma in the Ulten Zone of the Eastern Alps (Tumiati et al. 2003). Although Hauzenberger et al. (1996) obtained a WR–garnet Sm–Nd isochron of 351±1 Ma from the Ulten stromatic gneisses (garnet–kyanite paragneiss), it was interpreted as the age of Variscan high-grade metamorphism. Interestingly, Del Moro et al. (1999) presented Rb–Sr isotopic data from identical stromatic gneisses that scattered along a reference isochron of 330 Ma, which was interpreted as migmatization connected with intrusion of the Hercynotype plutons in the Alps. The two-stage evolution of the high-pressure paragneisses of the Variscan Ulten Zone, which confirmed monazite *in situ* U–Th–Pb data by LA–ICP-MS (Langone et al. 2011) with the old ages of 351–343 Ma (Mnz-I – shielded by garnet), has been related to a prograde stage of the Variscan metamorphic evolution, while the younger ages of 330–326 Ma (Mnz-II – small matrix monazites and porphyroblasts) were related to the thermal metamorphic peak and migmatization of the entire Ulten Zone. However, the Variscan metamorphism in the Alps seems to be coeval or even younger than the widespread Variscan granitic magmatism, thus causing a regional contact-metamorphism and elevated heat flow (Schaltegger & Gebauer 1999).

The MP metamorphism in the Bohemian Massif is well-documented by Lu–Hf WR–garnet dating with ages of 344.5 ±1.3 and 342±7 Ma, and SIMS monazite U–Pb results with an age of 341±3 Ma of the garnet-bearing micaschists from the Krkonoše–Jizera Massif of the Saxothuringian Domain (Konopásek et al. 2019). However, Kröner et al. (2000) proposed that U–Th–Pb SHRIMP zircon data from granulites of the Moldanubian Zone (southern Bohemian Massif) with an age of ca. 340 Ma, together with identical data from the cordierite-bearing melt, may indicate decompression and/or the medium to low pressure granulite facies stages. A similar scenario was confirmed as well by Friedl et al. (2011) for the Dunkelsteiner Wald granulites (Moldanubian Zone, Bohemian Massif), obtaining the coeval SHRIMP zircon concordia ages of 342–337 Ma. Monazite *in situ* U–Th–Pb geochronology in the Erzgebirge Crystalline Complex (Saxothuringian Zone) on phyllites and micaschists surrounding the UHP core of the Erzgebirge dome revealed that the hanging-wall phyllites experienced prograde metamorphism at ca. 350 Ma, followed by exhumation at ca. 345–340 Ma (Jouvent et al. 2023). Interestingly, the MP amphibolite-facies retrogression at ca. 350–330 Ma occurred in various units (zones) of the Bohemian Massif (Lardeaux et al. 2014 and references therein), which was caused by extensive granitic magmatism within the European Variscides.

When summarizing the above-presented work, it is obvious that the HP eclogite facies metamorphism from the Tatra Mts. at ca. 355 Ma has analogues in the Alps (the Ötztal Nappe and Silvretta Nappe) and the HP (UHP) second phase in the Bohemian Massif. Similarly, the MP (MP/HT) metamorphic event from the Tatra Mts. at about 346 Ma in the sillimanite-bearing gneisses and migmatites correspondingly reflects the situation in the metapelitic middle crust in the Alps and the Bohemian Massif.

The collision zone extending from the stable European Variscides to the Western Carpathians can be identified by the occurrence of eclogites in the Tatra Mts. and some other pre-Alpine basement complexes of the Western Carpathians (Janák et al. 2007; Faryad et al. 2020). However, the pre-Alpine basement of the Western Carpathians has been affected by Alpine tectonic events, and its original position and connection to the Variscan orogenic belt in Europe is uncertain. Similarities to the Bohemian Massif have been proposed (Moussallam et al. 2012), suggesting an eastern extension of the Moldanubian zone. Alternatively, Neubauer et al. (2022) suggested that the Variscan collision zone spread from the Eastern Alps to the Western and Southern Carpathians, as Late Devonian–Carboniferous plate convergence led to subduction of the Paleo-Adria margin underneath the accreted Variscan convergence belt.

Generally, the high-pressure metamorphism was accompanied by stacking of nappe sheets during continental subduction/collision processes in the Variscan Europe. The continuous return of deep crustal material from the subduction channel after maximum of the crustal-stacking was associated consequently with extension and crustal thinning. This led to a juxtaposition of rock units that were metamorphosed at different depths and in different periods of the lifetime of the continental subduction/collision zone, thus suggesting at least a 10 Myr when the originally deeper eclogites reached the hot migmatized gneisses in the middle crustal level in the Tatra Mts.

**Acknowledgments:** This work was financially supported from the Slovak Research and Development Agency: Grant APVV-18-0107, and VEGA-2/0056/20. M. Boczkowska and R. Anczkiewicz acknowledge funding from the internal IGS PAS grant and EPOS PL+ grant from the Ministry of Education. We thank Marian Janák for providing part of the samples for this study, as well as for long-term discussion of the Tatra Mts. tectono-metamorphic evolution and overall support. Constructive reviews and valuable comments by Matthijs Smit and an anonymous reviewer helped to improve the manuscript; Igor Broska is thanked for editorial handling.

## References

Ackerman L., Bizimis M., Haluzová E., Sláma J., Svojtka M., Hirajima T. & Erban V. 2016: Re–Os and Lu–Hf isotopic constraints on the formation and age of mantle pyroxenites from the Bohemian Massif. *Lithos* 256, 197–210. https://doi.org/10.1016/j.lithos.2016.03.023

Anczkiewicz R., Platt J.P., Thirlwall M.F. & Wakabayashi J. 2004: Franciscan subduction off to a slow start: evidence from high-precision Lu–Hf garnet ages on high grade-blocks. *Earth and Planetary Science Letters* 225, 147–161. https://doi.org/10.1016/j.epsl.2004.06.003

Anczkiewicz R., Szczepański J., Mazur S., Storey C., Crowley Q., Villa I.M., Thirlwall M.F. & Jeffries T.E. 2007: Lu–Hf geochronology and trace element distribution in garnet: implications for uplift and exhumation of ultra-high pressure granulites in the Sudetes, SW Poland. *Lithos* 95, 363–380. https://doi.org/10.1016/j.lithos.2006.09.001

Anczkiewicz R., Thirlwall M., Alard O., Rogers N.W. & Clark C. 2012: Diffusional homogenization of light REE in garnet from the Day Nui Con Voi Massif in N-Vietnam: Implications for Sm–Nd geochronology and timing of metamorphism in the Red River shear zone. *Chemical Geology* 318, 16–30. https://doi.org/10.1016/j.chemgeo.2012.04.024

Andrusov D. 1968: Grundriss der Tektonik der Nördlichen Karpaten. *Veda Publishing House of SAS*, Bratislava.

Bagdasaryan G.P., Cambel B., Veselský J. & Gukasyan R.C. 1977: Potassium–Argon age determination of the Western Carpathians crystalline basement rocks and Preliminary interpretation of the results. *Geologica Carpathica* 28, 219–242 (in Russian with English abstract).

Bagdasaryan G.P., Gukasyan R.C., Cambel B. & Veselský J. 1983: The Rb–Sr age determination results of the metamorphic rocks from the Malé Karpaty Mts. crystalline basement. *Geologica Carpathica* 34, 387–397 (in Russian with English abstract).

Broska I., Janák M., Svojtka M., Yi K., Konečný P., Kubiš M., Kurylo S., Hrdlička M. & Maraszewsk, M. 2022: Variscan granitic magmatism in the Western Carpathians with linkage to slab breakoff. *Lithos* 412–413. https://doi.org/10.1016/j.lithos.2021.106589

Brown M. & Johnson T. 2018: Secular change in metamorphism and the onset of global plate tectonics. *American Mineralogist* 103, 181–196. https://doi.org/10.2138/am-2018-6166

Burda J., Gawęda A. & Klötzli U. 2013a: Geochronology and petrogenesis of granitoid rocks from the Goryczkowa Unit, Tatra Mountains (Central Western Carpathians). *Geologica Carpathica* 64, 419–435. https://doi.org/10.2478/geoca-2013-0029

Burda J., Gawęda A. & Klötzli U. 2013b: U–Pb zircon age of the youngest magmatic activity in the High Tatra granites (Central Western Carpathians). *Geochronometria* 40, 134–144. https://doi.org/10.2478/s13386-013-0106-9

Burda J., Klötzli U., Majka J., Chew D., Li Q-L., Liu Y., Gawęda A. & Wiedenbeck M. 2021: Tracing proto-Rheic – Qaidam Ocean vestiges into the Western Tatra Mountains and implications for the Palaeozoic palaeogeography of Central Europe. *Gondwana Research* 91, 188–204. https://doi.org/10.1016/j.gr.2020.12.016

Catlos E.J., Broska I., Kohút M., Etzel T.M., Kyle J.R., Stockli D.F., Miggins D.P. & Campos D. 2022: Geochronology, geochemistry, and geodynamic evolution of Tatric granites from crystallization to exhumation (Tatra Mountains, Western Carpathians). *Geologica Carpathica* 73, 517–544. https://doi.org/10.31577/GeolCarp.73.6.1

Chang R., Neubauer F., Liu Y., Genser J., Yuan S., Huang Q., Li W. & Yu S. 2022: Protolith and metamorphic age of the Sieggraben Eclogites: Implications for the Permian to Cretaceous Wilson cycle in the Austroalpine unit. *Lithos* 434, 106923. https://doi.org/10.1016/j.lithos.2022.106923

Chang R., Neubauer F., Liu Y., Genser J., Guan Q., Huang Q. & Yuan S. 2023: Permian to Triassic protolith ages of type locality eclogites in the Eastern Alps: Implications for the opening of the Meliata back-arc basin. *Geology* 51, 537–542. https://doi.org/10.1130/G50903.1

Chowdhury P., Chakraborty S. & Gerya T.V. 2021: Time will tell: Secular change in metamorphic timescales and the tectonic implications. *Gondwana Research* 93, 291–310. https://doi.org/10.1016/j.gr.2021.02.003

Collett S., Štípská P., Schulmann K., Peřestý V., Soldner J., Anczkiewicz R., Lexa O. & Kylander-Clark A. 2018: Combined Lu–Hf and Sm–Nd geochronology of the Mariánské Lázně Complex: New constraints on the timing of eclogite-and granulite-facies metamorphism. *Lithos* 304, 74–94. https://doi.org/10.1016/j.lithos.2018.02.007

Dallmeyer D.R., Neubauer F., Handler R., Fritz H., Müller W., Pana D. & Putiš M. 1996: Tectonothermal evolution of internal Alps and Carpathians: Evidence from $^{40}Ar/^{39}Ar$ mineral and whole-rock data. *Eclogae Geologicae Helvetiae* 89, 203–227.

Del Moro A., Sassi F.P. & Zirpoli G. 1980: Preliminary results on the radiometric age of the Hercynian metamorphism in the South-Alpine basement of the Eastern Alps. *Neues Jahrbuch für Geologie und Paläontologie – Monatshefte* 12, 707–718. https://doi.org/10.1127/njgpm/1980/1981/707

Del Moro A., Martin S. & Prosser G. 1999: Migmatites of the Ulten zone (NE Italy), a record of melt transfer in deep crust. *Journal of Petrology* 40, 1803–1826. https://doi.org/10.1093/petroj/40.12.1803

Dewey J.F. & Burke K.C. 1973: Tibetan, Variscan, and Precambrian basement reactivation: products of continental collision. *The Journal of Geology* 81, 683–692. https://doi.org/10.1086/627920

Duchêne S., Blichert-Toft J., Luais B., Télouk P., Lardeaux J.M. & Albarède F. 1997: The Lu–Hf dating of garnets and the ages of the Alpine high-pressure metamorphism. *Nature* 387, 586–589. https://doi.org/10.1038/42446

England P.C. & Thompson A.B. 1984: Pressure–temperature–time paths of regional metamorphism I. Heat transfer during the evolution of regions of thickened continental crust. *Journal of Petrology* 25, 894–928. https://doi.org/10.1093/petrology/25.4.894

Faryad S.W., Ivan P. & Jacko S. 2005: Metamorphic petrology of metabasites from the Branisko and Čierna Hora Mountains (Western Carpathians, Slovakia). *Geologica Carpathica* 56, 3–16.

Faryad S.W., Ivan P. & Jedlicka R. 2020: Pre-Alpine high-pressure metamorphism in the Gemer unit: mineral textures and their geodynamic implications for Variscan Orogeny in the Western Carpathians. *International Journal of Earth Sciences* 109, 1547–1564. https://doi.org/10.1007/s00531-020-01856-2

Friedl G., Cooke R.A., Finger F., McNaughton N.J. & Fletcher I.R. 2011: Timing of Variscan HP–HT metamorphism in the Moldanubian Zone of the Bohemian Massif: U–Pb SHRIMP dating on multiply zoned zircons from a granulite from the Dunkelsteiner Wald Massif, Lower Austria. *Mineralogy and Petrology* 102, 63–75. https://doi.org/10.1007/s00710-011-0162-x

Fritz H., Neubauer F., Janák M. & Putiš M. 1992: Variscan mid-crustal thrusting in the Carpathians II: Kinematics and fabric evolution of the Western Tatra basement. *Terra Abstracts*, Supplement 2 to *Terra Nova* 4, 24.

Froitzheim N., Plašienka D. & Schuster R. 2008: Alpine tectonics of the Alps and Western Carpathians. In: McCann T. (Ed.): The geology of central Europe, Mesozoic and Cenozoic (Vol. 2), *Geological Society Publishing House*, London, 1141–1232. https://doi.org/10.1144/CEV2P.6

Gawęda A., Burda J., Klötzli U., Golonka J. & Szopa K. 2016: Episodic construction of the Tatra granitoid intrusion (Central Western Carpathians, Poland/Slovakia): consequences for the geodynamics of Variscan collision and Rheic Ocean closure. *International Journal of Earth Sciences* 105, 1153–1174. https://doi.org/10.1007/s00531-015-1239-2

Gawęda A., Burda J., Golonka J., Klötzli U., Chew D., Szopa K. & Wiedenbeck M. 2017: The evolution of eastern Tornquist-Paleoasian Ocean and subsequent continental collisions: A case study from the Western Tatra Mountains, Central Western Carpathians (Poland). *Gondwana Research* 48, 134–152. https://doi.org/10.1016/j.gr.2017.04.021

Gawęda A., Szopa K., Chew D., O'Sullivan G.J., Burda J., Klötzli U. & Golonka J. 2018: Variscan post-collisional cooling and uplift of the Tatra Mountains crystalline block constrained by integrated zircon, apatite and titanite LA-(MC)-ICP-MS U–Pb dating and rare earth element analyses. *Chemical Geology* 484, 191–209. https://doi.org/10.1016/j.chemgeo.2018.03.012

Gorek A. 1959: An outline of geological and petrographical relationships in the Crystalline complexes of the Tatra Mts. *Geologický Zborník SAV* 10, 13–88.

Hauke M., Froitzheim N., Nagel T.J., Miladinova I., Fassmer K., Fonseca R.O., Sprung P. & Münker C. 2019: Two high-pressure metamorphic events, Variscan and Alpine, dated by Lu–Hf in an eclogite complex of the Austroalpine nappes (Schobergruppe, Austria). *International Journal of Earth Sciences* 108, 1317–1331. https://doi.org/10.1007/s00531-019-01708-8

Hauzenberger C.A., Höller W. & Hoinkes G. 1996: Transition from eclogite to amphibolite-facies metamorphism in the Austroalpine Ulten Zone. *Mineralogy and Petrology* 58, 111–130. https://doi.org/10.1007/BF01172092

Hoinkes G., Thöni M., Lichem C., Bernhard F., Kaindl R., Schweigl J., Troper P. & Cosca M. 1997: Metagranitoids and associated metasediments as indicators for the pre-Alpine magmatic and metamorphic evolution of the western Austroalpine Ötztal Basement (Kaunertal, Tirol). *Schweizerische Mineralogische Petrographische Mittailungen* 77, 299–314. https://doi.org/10.5169/seals-58486

Janák M. 1993: Calc-silicate metamorphic rocks of the High Tatra crystalline basement. *Mineralia Slovaca* 25, 177–182.

Janák M. 1994: Variscan uplift of the crystalline basement, Tatra Mts., Central Western Carpathians: evidence from $^{40}Ar/^{39}Ar$ laser probe dating of biotite and *P–T–t* paths. *Geologica Carpathica* 45, 293–300.

Janák M. & Lupták B. 1997: Pressure-temperature conditions of high-grade metamorphism and migmatitization in the Malá Fatra crystalline complex, the Western Carpathians. *Geologica Carpathica* 48, 287–302.

Janák M., O'Brien P.J., Hurai, V. & Reutel C., 1996. Metamorphic evolution and fluid composition of garnet-clinopyroxene amphibolites from the Tatra Mountains, Western Carpathians. *Lithos* 39, 57–79. https://doi.org/10.1016/S0024-4937(96)00019-9

Janák M., Hurai V., Ludhová L., O´Brien P.J. & Horn E.E. 1999: Dehydration melting and devolatilization of high-grade metapelites: the Tatra Mountains, Western Carpathians. *Journal of Metamorphic Geology* 17, 379–396. https://doi.org/10.1046/j.1525-1314.1999.00206.x

Janák M., Méres Š. & Ivan P. 2007: Petrology and metamorphic *P–T* conditions of eclogites from the northern Veporic Unit (Western Carpathians, Slovakia). *Geologica Carpathica* 58, 121–131.

Janák M., Mikuš T., Pitoňák P. & Spišiak J. 2009: Eclogites overprinted in the granulite facies from the Ďumbier crystalline complex (Low Tatra Mountains, Western Carpathians). *Geologica Carpathica* 60, 193–204. https://doi.org/10.2478/v10096-009-0013-4

Janák M., Petrík I., Konečný P., Kurylo S., Kohút M. & Madarás J. 2022: Variscan metamorphism and partial melting of sillimanite-bearing metapelites in the High Tatra Mts. constrained by Th–U–Pb dating of monazite. *Geologica Carpathica* 73, 97–122. https://doi.org/10.31577/GeolCarp.73.2.1

Jochum K.P., Weis U., Stoll B., Kuzmin D., Yang Q., Raczek I., Jacob D.E., Stracke A., Birbaum K., Frick D.A., Günther D. & Enzweiler J. 2011: Determination of reference values for NIST SRM 610-617 glasses following ISO guidelines. *Geostandards and Geoanalytical Research* 35, 397–429. https://doi.org/10.1111/j.1751-908X.2011.00120.x

Jouvent M., Peřestý V., Jeřábek P., Lexa O. & Kylander-Clark, A.R.C. 2023: Assembly of the Variscan orogenic wedge in the Bohemian Massif: Monazite U–Pb geochronology of the tectonic events recorded in Saxothuringian metasediments. *Tectonics* 42, e2022TC007626. https://doi.org/10.1029/2022TC007626

Kahan Š. 1969: Eine neue Ansicht über den geologischen Aufbau des Kristallinikums der West Tatra. *Acta Geologica et Geographica Universitatis Comenianae* 12, 115–122.

Kohút M. & Janák M. 1994: Granitoids of the Tatra Mts., Western Carpathians: field relationships and petrogenetic implications. *Geologica Carpathica* 45, 301–311.

Kohút M. & Larionov A.N. 2021: From subduction to collision: Genesis of the Variscan granitic rocks from the Tatric Superunit (Western Carpathians, Slovakia). *Geologica Carpathica* 72, 96–113. https://doi.org/10.31577/GeolCarp.72.2.2

Kohút M. & Sherlock S.C. 2003: Laser microprobe $^{40}Ar–^{39}Ar$ analysis of pseudotachylyte and host-rocks from the Tatra Mountains, Slovakia: evidence for late Palaeogene seismic/tectonic activity. *Terra Nova* 15, 417–424. https://doi.org/10.1046/j.1365-3121.2003.00514.x

Konopásek J., Anczkiewicz R., Jeřábek P., Corfu F. & Žáčková E. 2019: Chronology of the Saxothuringian subduction in the West Sudetes (Bohemian Massif, Czech Republic and Poland). *Journal of the Geological Society London* 176, 492–504. https://doi.org/10.1144/jgs2018-173

Kröner A., O'brien P.J., Nemchin A.A. & Pidgeon R.T. 2000: Zircon ages for high pressure granulites from South Bohemia, Czech Republic, and their connection to Carboniferous high temperature processes. *Contributions to Mineralogy and Petrology* 138, 127–142. https://doi.org/10.1007/s004100050013

Ladenhauf C., Armstrong R., Konzett J. & Miller C. 2001: The timing of pre-Alpine high-pressure metamorphism in the Eastern Alps: constraints from U–Pb SHRIMP dating of eclogite zircons from the Austroalpine Silvretta nappe. *Journal of Conference Abstracts* 6, 600.

Langone A., Braga R., Massonne H.-J. & Tiepolo M. 2011: Preservation of old (prograde metamorphic) U–Th–Pb ages in unshielded monazite from the high-pressure paragneisses of the Variscan Ulten Zone (Italy). *Lithos* 127, 68–85. https://doi.org/10.1016/j.lithos.2011.08.007

Lapen T.J., Johnson C.M., Baumgartner L.P., Mahlen N.J., Beard B.L. & Amato J.M. 2003: Burial rates during prograde metamorphism of an ultra-high-pressure terrane: an example from Lago di Cignana, western Alps, Italy. *Earth and Planetary Science Letters* 215, 57–72. https://doi.org/10.1016/S0012-821X(03)00455-2

Lardeaux J.M., Schulmann K., Faure M., Janoušek V., Lexa O., Skrzypek E., Edel J.B. & Štípská P. 2014: The Moldanubian zone in the French Massif Central, Vosges/Schwarzwald and Bohemian Massif revisited: differences and similarities. *Geological Society, London*, *Special Publications* 405, 7–44. https://doi.org/10.1144/SP405.14

Ludwig K.R. 2008: Isoplot. A Geochronological Toolkit for Microsoft Excel. *Berkley Geochronology Centre*, Special Publication 4.

Lugmair G.W. & Marti K. 1978: Lunar initial $^{143}Nd/^{144}Nd$: differential evolution of the lunar crust and mantle. *Earth and Planetary Science Letters* 39, 349–357. https://doi.org/10.1016/0012-821X(78)90021-3

Maierová P., Schulann K., Lexa O., Guillot S., Štípská P., Janoušek V. & Čadek O. 2016: European Variscan orogenic evolution as an analogue of Tibetan-Himalayan orogen: Insights from petrology and numerical modeling. *Tectonics* 35, 1760–1780. https://doi.org/10.1002/2015TC004098

Maluski H., Rajlich P. & Matte P. 1993: $^{40}Ar–^{39}Ar$ dating of the Inner Carpathians Variscan basement and Alpine mylonitic overprinting. *Tectonophysics* 223, 313–337. https://doi.org/10.1016/0040-1951(93)90143-8

Maraszewska M., Broska I., Kohút M., Yi K-W., Konečný P. & Kurylo S. 2022: The Ďumbier–Prašivá High K calc-alkaline granite suite (Low Tatra Mts., Western Carpathians): insights into their evolution from geochemistry and geochronology. *Geologica Carpathica* 73, 273–291. https://doi.org/10.31577/GeolCarp.73.4.1

Medaris L.G., Beard B.L. & Jelínek E. 2006: Mantle-derived, UHP garnet pyroxenite and eclogite in the Moldanubian Gföhl Nappe, Bohemian Massif: A geochemical review, new PT determinations, and tectonic interpretation. *International Geological Reviews* 48, 765–777. https://doi.org/10.2747/0020-6814.48.9.765

Meli S. 2004: Rb–Sr and $^{40}Ar/^{39}Ar$ age constraints on the Variscan metamorphism recorded by Ordovician acidic metavolcanic rocks in the Eastern Southalpine basement. *Rendiconti Lincei di Scienze Fisiche e Naturali* 15, 205–223. https://doi.org/10.1007/BF02904461

Miladinova I., Froitzheim N., Nagel T.J., Janák M., Fonseca R.O., Sprung P. & Münker C. 2022: Constraining the process of intracontinental subduction in the Austroalpine Nappes: Implications from petrology and Lu–Hf geochronology of eclogites. *Journal of Metamorphic Geology* 40, 423–456. https://doi.org/10.1111/jmg.12634

Miller C. & Thöni M. 1995: Origin of eclogites from the Austroalpine Ötztal basement (Tirol, Austria): geochemistry and Sm–Nd vs. Rb–Sr isotope systematics. *Chemical Geology* 122, 199–225. https://doi.org/10.1016/0009-2541(95)00033-I

Miller C. & Thöni M. 1997: Eo-Alpine eclogitisation of Permian MORB-type gabbros in the Koralpe (Eastern Alps, Austria): new geochronological, geochemical and petrological data. *Chemical Geology* 137, 283–310. https://doi.org/10.1016/S0009-2541(96)00165-9

Moussallam Y., Schneider D.A., Janák M., Thöni M. & Holm D.K. 2012: Heterogeneous extrusion and exhumation of deep-crustal Variscan assembly: Geochronology of the Western Tatra Mountains, northern Slovakia. *Lithos* 144, 88–108. https://doi.org/10.1016/j.lithos.2012.03.025

Neubauer F., Liu Y., Dong Y., Chang R., Genser J. & Yuan S. 2022: Pre-Alpine tectonic evolution of the Eastern Alps: from prototethys to paleotethys. *Earth-Science Reviews* 226, 103923. https://doi.org/10.1016/j.earscirev.2022.103923

O'Brien P.J. 1997: Garnet zoning and reaction textures in overprinted eclogites, Bohemian Massif, European Variscides: a record of their thermal history during exhumation. *Lithos* 41, 119–133. https://doi.org/10.1016/S0024-4937(97)82008-7

Paton C., Hellstrom J., Paul B., Woodhead J. & Hergt J. 2011: Iolite: Freeware for the visualisation and processing of mass spectrometric data. *Journal of Analytical Atomic Spectrometry* 26, 2508–2518. https://doi.org/10.1039/C1JA10172B

Plašienka D. 2018: Continuity and Episodicity in the Early Alpine Tectonic Evolution of the Western Carpathians: How Large-Scale Processes Are Expressed by the Orogenic Architecture and Rock Record Data. *Tectonics* 37, 2029–2079. https://doi.org/10.1029/2017TC004779

Poller U. & Todt W. 2000: U–Pb single zircon data of granitoids from the High Tatra Mountains (Slovakia): implications for the geodynamic evolution. *Transactions of the Royal Society of Edinburgh Earth Sciences* 91, 235–243. https://doi.org/10.1017/S0263593300007409

Poller U., Janák M., Kohút M. & Todt W. 2000: Early Variscan magmatism in the Western Carpathians: U–Pb zircon data from granitoids and orthogneisses of the Tatra Mountains (Slovakia). *International Journal of Earth Sciences* 89, 336–349. https://doi.org/10.1007/s005310000082

Poller U., Huth J., Hoppe P. & Williams I.S. 2001: REE, U, Th, and Hf distribution in zircon from Western Carpathian Variscan granitoids: a combined cathodoluminescence and ion microprobe study. *American Journal of Science* 301, 858–867. https://doi.org/10.2475/ajs.301.10.858

Putiš M., Ivan P., Kohút M., Spišiak J., Siman P., Radvanec M., Uher P., Sergeev S., Larionov A., Méres S., Demko R. & Ondrejka M. 2009: Meta-igneous rocks of the West-Carpathian basement, Slovakia: indicators of Early Paleozoic extension and shortening events. *Bulletin de la Société géologique de France* 180, 461–471. https://doi. org/10. 2113/gssgfbull.180.6. 461

Schaltegger U. & Gebauer D. 1999: Pre-Alpine geochronology of the Central, Western and Southern Alps. *Schweizerische Mineralogische Petrographische Mittailungen* 79, 79–87.

Scherer E.E., Cameron K.L. & Blichert-Toft J. 2000: Lu–Hf garnet geochronology: Closure temperature relative to the Sm–Nd system and the effects of trace mineral inclusions. *Geochimica et Cosmochimica Acta* 64, 3413–3432. https://doi.org/10.1016/S0016-7037(00)00440-3

Schmädicke E., Will T.M., Ling X., Li X.H. & Li Q.L. 2018: Rare peak and ubiquitous post-peak zircon in eclogite: Constraints for the timing of UHP and HP metamorphism in Erzgebirge, Germany. *Lithos* 322, 250–267. https://doi.org/10.1016/j.lithos.2018.10.017

Schulz B. 2021. Petrochronology of Monazite-Bearing Garnet Micaschists as a Tool to Decipher the Metamorphic Evolution of the Alpine Basement. *Minerals* 11, 981. https://doi.org/10.3390/min11090981

Smit M., Scherer E. & Mezger K. 2013: Lu–Hf and Sm–Nd garnet geochronology: chronometric closure and implications for dating petrological processes. *Earth and Planetary Science Letters* 381, 222–233. https://doi.org/10.1016/j.epsl.2013.08.046

Thirlwall M.F. & Anczkiewicz R. 2004: Multidynamic isotope ratio analysis using MC–ICP–MS and the causes of secular drift in Hf, Nd and Pb isotope ratios. *International Journal of Mass Spectrometry* 235, 59–81. https://doi.org/10.1016/j.ijms.2004.04.002

Thöni M. & Jagoutz E. 1992: Some new aspects of dating eclogites in orogenic belts: Sm–Nd, Rb–Sr, and Pb–Pb isotopic results from the Austroalpine Saualpe and Koralpe type-locality (Carinthia/Styria, southeastern Austria). *Geochimica et Cosmochimica Acta* 56, 347–368. https://doi.org/10.1016/0016-7037(92)90138-9

Tumiati S., Thöni M., Nimis P., Martin S. & Mair V. 2003: Mantle–crust interactions during Variscan subduction in the Eastern Alps (Nonsberg–Ulten zone): geochronology and new petrological constraints. *Earth and Planetary Science Letters* 210, 509–526. https://doi.org/10.1016/S0012-821X(03)00161-4

Warren C.J. 2013: Exhumation of (ultra-)high-pressure terranes: concepts and mechanisms. *Solid Earth* 4, 75–92. https://doi.org/10.5194/se-4-75-2013

**Electronic supplementary material** is available online:
Supplementary Table S1 at http://geologicacarpathica.com/data/files/supplements/GC-74-5-Kohut_TableS1.docx
Supplementary Fig. S1 at http://geologicacarpathica.com/data/files/supplements/GC-74-5-Kohut_FigS1.jpg